Comment on “Electromagnetic force on structured metallic surfaces”

Demeng Feng, Raymond A. Wambold, Yuzhe Xiao, Chenghao Wan, Zhaoning Yu, Victor W. Brar, and Mikhail A. Kats

Phys. Rev. B **105**, 207401 — Published 27 May 2022

DOI: 10.1103/PhysRevB.105.207401

Comment on "Electromagnetic force on structured metallic surfaces"

Demeng Feng[1], Raymond A. Wambold[1], Yuzhe Xiao[1], Chenghao Wan[1,2], Zhaoning Yu[1,3], Victor W. Brar[2,3], Mikhail A. Kats[1,2,3]

[1]Department of Electrical and Computer Engineering, University of Wisconsin – Madison, Madison, WI 53706, USA

[2]Department of Materials Science and Engineering, University of Wisconsin – Madison, Madison, WI 53706, USA

[3]Department of Physics, University of Wisconsin – Madison, Madison, WI 53706, USA

Abstract

In [A. H. Velzen and K. J. Webb, Phys. Rev. B **92**, 115416 (2015)], Velzen and Webb proposed that by structuring a metal film suspended in free space with a periodic array of nanoscale slots, the steady state optical pressure on the film resulting from an incident plane wave can be substantially enhanced compared to the standard radiation-pressure limit. This result appears to be in violation of the law of momentum conservation, given that the momentum of free-space electromagnetic plane waves is well established. We recalculated the optical fields and forces for the same configuration as Velzen and Webb and found that, although the calculated optical fields and force densities agree with the published result, the resulting total optical forces were not enhanced and instead matched the standard radiation-pressure relation. Our calculations imply that the diverging results arise due to different choices of the region used for integration of the force density.

In [1], the authors proposed that the steady-state force that a light beam imparts to a metallic object in free space can be dramatically enhanced by structuring the surface with a periodic array of slots. Specifically, the authors explored a gold (Au) film with periodic grooves illuminated by a plane wave (**Fig. 1(a)**) and found that the optical pressure exceeded the conventional radiation-pressure limit by more than an order of magnitude. The proposed mechanism for this effect is the large spatial variation of the electric field just inside the metal at wavelengths close to the plasmonic resonances of the structure. Follow-up papers have explored such force enhancement both theoretically [2] [3] [4] and experimentally [5].

Our interpretation is that the results reported in ref. [1] are inconsistent with the conservation of momentum. According to conventional electromagnetic (EM) theory, the optical pressure p on an opaque, macroscopic object floating in free space illuminated by a plane wave and reflecting specularly (i.e., no far-field diffraction orders or scattering) is [6]

$$p = \frac{S(1+|\Gamma|^2)}{c} \tag{1}$$

where c is the speed of light and S is the magnitude of the time-averaged Poynting vector (i.e., the intensity) of the incident light. $|\Gamma|^2$ is the reflectance, defined as $|\Gamma|^2 = \frac{S_r}{S}$, where S_r is the intensity of the reflected wave in the far field. Eqn. (1) indicates that the optical pressure increases with reflectance, and the theoretical maximum optical pressure is $2S/c$ for perfectly reflecting surfaces. This limit is associated with maximum momentum exchange between the object and incident photons. In the photon picture, the momentum of an incident photon in free space is h/λ_0, where λ_0 is the wavelength. The maximum momentum the photon can impart is $2h/\lambda_0$, when the photon is reflected in the opposite direction. Although the momentum of electromagnetic fields (or photons) inside materials has been a point of debate [6] [7], the momentum of electromagnetic waves in free space is well established.

Because the conclusions in ref. [1] are out of line with the aforementioned arguments based on the conservation of momentum, we sought to re-examine the findings of that work by reproducing the field simulation results and then recalculating the optical force densities and total forces, with the geometry and light source the same as Fig. 1(a) in ref. [1]. We find that the *total* optical force on the object is bounded by the $2S/c$ limit even as there can be large *local* force densities, especially when the structure is close to resonance.

Review and discussion of optical forces and force densities

As in ref. [1], we made assumed that, at optical frequencies, the magnetization of Au is zero ($\boldsymbol{M} = 0$) and, since there are no current sources other than the incident field, the external current density and external charge density are both zero.

We calculated the optical force using two different force-density formulations. The first is the Lorentz formulation, which under our assumptions has force density [8]:

$$\boldsymbol{f}_{\mathrm{L}} = \frac{\partial \boldsymbol{P}}{\partial t} \times \mu_0 \boldsymbol{H} - (\nabla \cdot \boldsymbol{P})\boldsymbol{E} \tag{2}$$

where $\boldsymbol{P}$ is the material polarization. The second is the Einstein-Laub (EL) formulation, which is what is used in ref. [1]. Under the same assumptions, the force-density expression in the EL formulation is [8]:

$$\boldsymbol{f}_{\mathrm{EL}} = \frac{\partial \boldsymbol{P}}{\partial t} \times \mu_0 \boldsymbol{H} + (\boldsymbol{P} \cdot \nabla)\boldsymbol{E} \tag{3}$$

Eqn. (3) is the same as Eqn. (2) in ref. [1]. Using Eqns. (2) and (3), the time-averaged total force on the object can then be calculated by integrating the time-averaged force density over region Ω (the "force-calculation region") that encompasses the object:

$$\langle \boldsymbol{F}_{\mathrm{L/EL}} \rangle = \iint_{\Omega} \langle \boldsymbol{f}_{\mathrm{L/EL}} \rangle \, dxdy \tag{4}$$

where $\langle \boldsymbol{F}_{\mathrm{L}} \rangle$ or $\langle \boldsymbol{F}_{\mathrm{EL}} \rangle$ are the time-averaged total forces in the Lorentz or EL formulation, respectively.

While Eqn. (4) provides a way to calculate the total optical force on an object, such calculations can be nontrivial when encountering sharp boundaries [9]. Boundary issues can be circumvented with the assistance of the stress tensors, which are associated with the force densities in the following way [8]:

$$\boldsymbol{f}_{\mathrm{L/EL}} = -\nabla \cdot \overleftrightarrow{\boldsymbol{T}}_{\mathrm{L/EL}} - \frac{\partial}{\partial t} \boldsymbol{g}_{\mathrm{L/EL}} \tag{5}$$

where

$$\overleftrightarrow{\boldsymbol{T}}_{\mathrm{L}} = \frac{1}{2}(\varepsilon_0 \boldsymbol{E} \cdot \boldsymbol{E} + \mu_0^{-1} \boldsymbol{B} \cdot \boldsymbol{B})\overleftrightarrow{\mathrm{I}} - \varepsilon_0 \boldsymbol{E}\boldsymbol{E} - \mu_0^{-1} \boldsymbol{B}\boldsymbol{B} \qquad \boldsymbol{g}_{\mathrm{L}} = \varepsilon_0 \boldsymbol{E} \times \boldsymbol{B}$$

$$\overleftrightarrow{\boldsymbol{T}}_{\mathrm{EL}} = \frac{1}{2}(\varepsilon_0 \boldsymbol{E} \cdot \boldsymbol{E} + \mu_0 \boldsymbol{H} \cdot \boldsymbol{H})\overleftrightarrow{\mathrm{I}} - \boldsymbol{D}\boldsymbol{E} - \boldsymbol{B}\boldsymbol{H} \qquad \boldsymbol{g}_{\mathrm{EL}} = \boldsymbol{E} \times \boldsymbol{H}/c^2$$

$\overleftrightarrow{\boldsymbol{T}}_{\mathrm{L}}$ is the Maxwell stress tensor (MST), $\overleftrightarrow{\boldsymbol{T}}_{\mathrm{EL}}$ is the EL stress tensor (EL tensor), $\boldsymbol{g}_{\mathrm{L}}$ is the EM momentum density in the Lorentz formulation (the Livens momentum density), and $\boldsymbol{g}_{\mathrm{EL}}$ is the momentum density in the EL formulation (the Abraham momentum density). $\boldsymbol{B}$ is $\mu_0(\boldsymbol{H} + \boldsymbol{M}) = \mu_0 \boldsymbol{H}$, since we assume $\boldsymbol{M} = 0$. $\overleftrightarrow{\mathrm{I}}$ is the identity second rank tensor, $\boldsymbol{D} = \epsilon_0 \boldsymbol{E} + \boldsymbol{P}$ is the displacement field, and $\boldsymbol{EE}$, $\boldsymbol{BB}$, $\boldsymbol{DE}$ and $\boldsymbol{BH}$ are dyadic products. We are aware that in refs. [10] [11], $\boldsymbol{g}_{\mathrm{EL}}$ is used rather than $\boldsymbol{g}_{\mathrm{L}}$ to get $\boldsymbol{f}_{\mathrm{L}}$ in Eqn. (5), We note, however, under the assumption $\boldsymbol{M} = 0$, there is no difference between $\boldsymbol{g}_{\mathrm{L}}$ and $\boldsymbol{g}_{\mathrm{EL}}$, and the expression of the Lorentz force density is the same as Eqn. (2) using either $\boldsymbol{g}_{\mathrm{L}}$ or $\boldsymbol{g}_{\mathrm{EL}}$. We use $\boldsymbol{g}_{\mathrm{L}}$ for $\boldsymbol{f}_{\mathrm{L}}$, following several textbooks [12] [13]. The total time-averaged force on an object within region Ω can be obtained as follows [14] [15]:

$$\langle \boldsymbol{F}_{\mathrm{L/EL}} \rangle = -\iint_{\Omega} \langle \nabla \cdot \overleftrightarrow{\boldsymbol{T}}_{\mathrm{L/EL}} \rangle \, dxdy = -\oint_{\partial\Omega} \langle \overleftrightarrow{\boldsymbol{T}}_{\mathrm{L/EL}} \rangle \cdot \mathrm{d}\boldsymbol{l} \tag{6}$$

where $d\boldsymbol{l} = dl \cdot \hat{\boldsymbol{n}}$ and $\hat{\boldsymbol{n}}$ is the normal vector for each boundary, Ω is the force-calculation region, and $\partial\Omega$ are the boundaries of Ω. Thus, Eqn. (4) with (2) or (3), and Eqn. (6) with $\overleftrightarrow{\boldsymbol{T}}_{\mathrm{L}}$ or $\overleftrightarrow{\boldsymbol{T}}_{\mathrm{EL}}$, give four different methods to calculate the time-averaged optical force on an object.

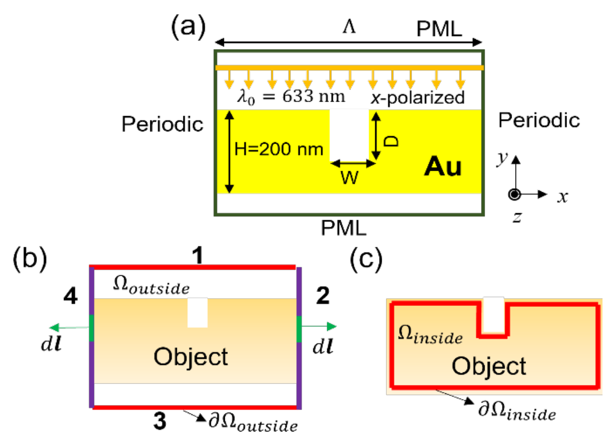

Fig. 1. (a) An Au film in free space with periodic slits on the top surface illuminated from the top. (b-c) Two choices of the force-calculation region Ω for the periodic structure. (b) Outside choice: ∂Ω consists of two segments in free space, and two segments that overlap the periodic boundaries. (c) Inside choice: ∂Ω are within the homogeneous object but as close as possible to the physical boundaries of the object.

We emphasize that selection of the force-calculation region Ω is crucial. The standard approach, e.g., used in refs. [14] [15] [16], is to have Ω fully enclose the object. If the object is periodic, it is impossible to fully enclose the object; however, the contributions to the stress tensor from two periodic boundaries cancel out.

Therefore, setting of $\partial\Omega$ as shown in **Fig. 1(b)** is equivalent to having $\partial\Omega$ in free space for a finite object. We refer to this as the "outside choice" ($\Omega_{outside}$). With $\Omega_{outside}$, if we calculate the time-averaged total force by integrating the force density (i.e., use Eqn. (2) or (3)), we integrate from inside the material, across material boundaries, and into the free-space background. If we use the stress tensor to calculate the time-averaged force (i.e., use Eqn. (6) with $\overleftrightarrow{\boldsymbol{T}}_{\mathrm{L}}$ or $\overleftrightarrow{\boldsymbol{T}}_{\mathrm{EL}}$), we integrate the stress tensor along $\partial\Omega_{outside}$ (boundary of $\Omega_{outside}$). Our understanding is that $\Omega_{outside}$ and $\partial\Omega_{outside}$ were not used in ref. [1]. Instead, the authors set $\partial\Omega$ within the homogeneous object but as close as possible to the physical boundary, as illustrated in **Fig. 1(c)**. We refer to this choice of Ω as the "inside choice" (Ω_{inside}). We show next that the inside choice can result in the appearance of force enhancement, as reported in ref. [1].

Calculation of fields, force densities, and total forces

We simulated the fields using the finite-difference time-domain (FDTD) method. As in ref. [1], the incident plane wave is x-polarized at a wavelength of $\lambda_0 = 633$ nm. We use $\epsilon_r = -11.835 + 1.241i$ for the relative permittivity of Au [17] and the period, Λ, is 400 nm. We set the intensity of the incident plane wave to 2 W/m^2, matching the parameters of Figs. 3, 5, and 6 in ref. [1] (Note that that there is a factor of two difference between our definition of power density and that of ref. [1], which can be seen for example by comparing Eqn. (1) with Eqn. (5) in ref. [1]). The slab was optically thick (H = 200 nm). **Fig. 2** shows the field simulation results for two slot depths (D = 55 and 75 nm) with W = 60 nm. Our calculated field distributions are essentially the same as Fig. 2 in ref. [1], though the ranges of the color bars are different because we used an incident power density to match Figs. 3, 5, and 6 in ref. [1], rather than Fig. 2.

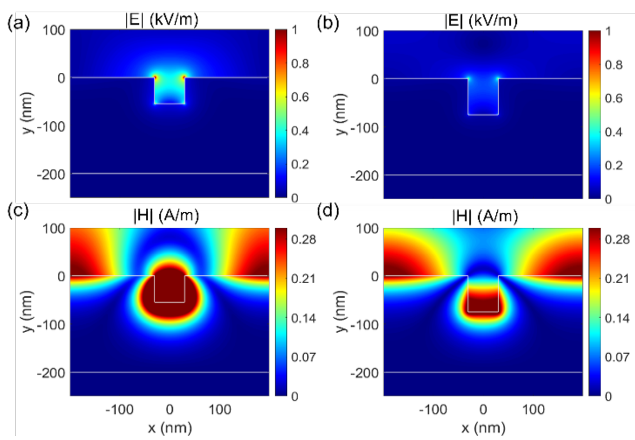

Fig. 2. **E** and **H** magnitudes for slot width W = 60 nm, and slot depths D = 55 nm (a & c), and 75 nm (b & d). The simulation mesh size is 0.25 nm.

We calculated the force-density distribution for two structures using the Lorentz and EL formulations, shown in **Fig. 3**. Note that the power density of the incident light used in **Fig. 3** is different from that what we used in **Fig. 2**; we chose the power density to be the same as what is used in Fig. 3 in ref. [1]. Our calculated force densities in the EL formulation match those in Fig. 3 in ref. [1], though there are minor discrepancies near resonance (here, D = 51 nm), likely due to different meshing. We note that the force-density distribution in the Lorentz formulation is somewhat different from that in the EL formulation, but we still expect the *total* optical force on the object be the same [8] [18] [19].

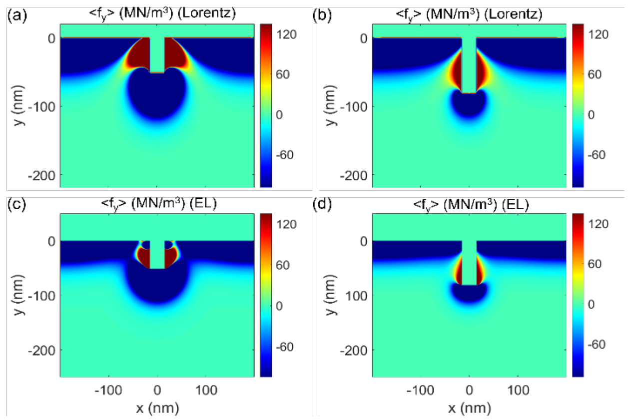

Fig. 3. The y-component of the calculated Lorentz (a-c) and EL (d-f) force densities for slot width W = 30 nm and slot depth D = 51 nm (a,c) and 81 nm (b,d). The power density of the incident light is 1 mW over a circular spot with diameter of 1 μm. The mesh size is 0.25 nm. For the Lorentz formulation, we calculated the force density within the object and across the material boundary. For the EL formulation, we only calculated the force density within the object.

Next, we calculated the macroscopic time-averaged pressure based on the field data, using three different approaches and $\Omega_{outside}$: Eqn. (4) with (2) ("volumetric Lorentz method"), Eqn. (6) with $\overleftrightarrow{\boldsymbol{T}}_{\mathrm{L}}$ ("MST method"), and Eqn. (6) with $\overleftrightarrow{\boldsymbol{T}}_{\mathrm{EL}}$ ("EL tensor method"). We also calculated the total optical force using Eqn. (1), based on the simulated far-field reflectance. These results are shown in **Fig. 4**. We found that the calculated pressure on a planar Au film is the same using each of the aforementioned methods (12.9 nN/m^2), and also matches the result in ref. [1]. For slot depth > 0, our results diverge from those of ref. [1]. Our calculations based on the MST method and the EL tensor method match those using Eqn. (1), with the maximum optical pressure never exceeding the theoretical limit of $2S/c = 13.3$ nN/m^2. Note that total calculated force is independent of the force-density formulation chosen. In summary, the large force enhancement described in ref. [1] does not appear in any of our calculations using $\Omega_{outside}$, which are all consistent with each other.

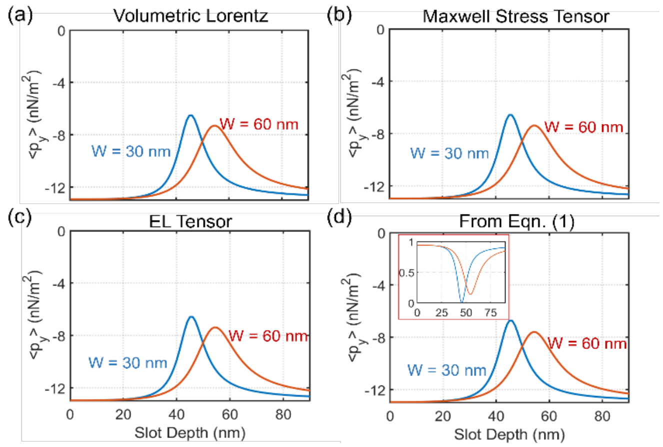

Fig. 4. Calculated time-averaged optical pressure as a function of slot depth based on (a) the volumetric Lorentz method (Eqn. (4) with (2)), (b) the MST method (Eqn. (6) with $\overleftrightarrow{\boldsymbol{T}}_{\mathrm{L}}$), (c) the EL tensor method (Eqn. (6) with $\overleftrightarrow{\boldsymbol{T}}_{\mathrm{EL}}$), and (d) Eqn. (1). In all cases, $\Omega = \Omega_{outside}$. The minus sign means that the direction of the optical force is in -*y* direction. The far-field reflectance as a function of slot depth is shown as an inset.

We note that boundaries where material properties change abruptly can cause difficulties for the integration and/or interpretation of the force density. First, the discontinuity of the *E*-field near abrupt material boundaries can result in delta-function-like peaks in the force density within one mesh cell of the boundary, which seems unphysical and can potentially cause trouble in numerical integration. This subtlety has been discussed in ref. [20] [21] [22]. Therefore, we believe that the total force results based on the MST method and the EL tensor method are more reliable. Second, the definition of $\boldsymbol{P}$ right at the object boundary is not clear to us, making the calculation of the term $(\boldsymbol{P} \cdot \nabla)\boldsymbol{E}$ at the object boundary difficult; for this reason, we did not use Eqn. (4) with (3) to calculate the total force using $\Omega_{outside}$. Note that this difficulty can be avoided when evaluating the force density in the Lorentz formulation, since we can convert Eqn. (2) using Maxwell's equations such that $\boldsymbol{f}_{\mathrm{L}}$ only depends on $\boldsymbol{E}$ and $\boldsymbol{H}$. We also note that, for some simple geometries, a rigorous analysis of force densities near material boundaries can be conducted and, in these cases, the integration of force densities can be performed without ambiguity [23] [24]. Finally, we note that a more rigorous treatment of material boundaries may require consideration of non-local effects [25] and other physics, which are beyond the scope of this comment.

The force density near object boundaries reveals the importance of the choice of Ω. As an illustration, we calculated the time-averaged optical pressure on the structure shown in **Fig. 1(a)** where W = 30 nm and D = 46 nm, using Eqns. (4) with (2) and (3), and Eqn. (6) with $\overleftrightarrow{\boldsymbol{T}}_{\mathrm{L}}$ and $\overleftrightarrow{\boldsymbol{T}}_{\mathrm{EL}}$, with $\Omega_{outside}$ and Ω_{inside} applied. Note that for Eqn. (4) with (3), we only performed the calculation using Ω_{inside}. These results are shown in **Fig. 5**. We find that using $\Omega_{outside}$, there is no force enhancement (at least using the Lorentz formulation).

However, using Ω_{inside}, an enhancement in the total force appears, though the Lorentz and EL formulations give different absolute forces. This apparent force enhancement is similar to what is shown in ref. [1].

We note that $\Omega_{outside}$ is widely used in the literature [16] [20] [26] [27] to calculate the total optical force exerted on the object, and refs. [14] [15] suggest that the using Ω_{inside} misses the force exerted on the object boundary, which means that the inside choice of Ω only calculates the local optical force exerted on *parts of* the object (i.e., local forces), not the *total* force exerted on the object. Although the local force can exceed the radiation pressure limit $2S/c$, the total force must be bounded by that limit, which comes from the conservation of momentum for the whole system (i.e., the object and incident and reflected photons).

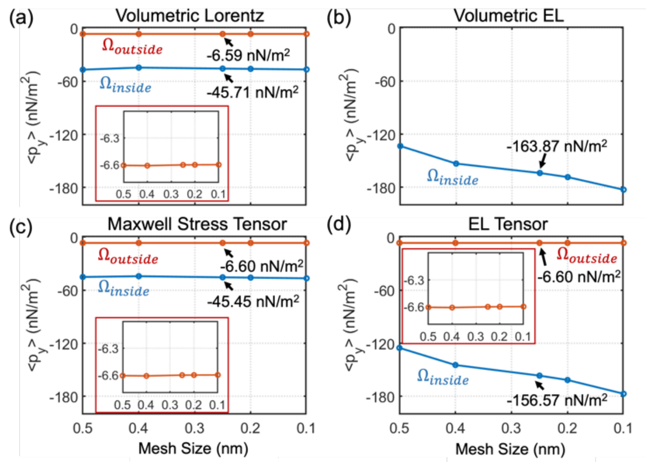

Fig. 5. Total time-averaged optical pressure on the structure in **Fig. 1** (with W = 30 nm and D = 46 nm), calculated using (a) the volumetric Lorentz method, (b) the volumetric EL method, (c) the MST method, and (d) the EL Tensor method, with both $\Omega_{outside}$ and Ω_{inside} applied, as a function of simulation mesh size. For panels (a), (c), (d), we show the zoomed-in plots of the results using $\Omega_{outside}$ to demonstrate convergence.

To further validate our calculations, we considered the optical pressure on a nanostructured Au film with finite size in the *x*-direction (**Fig. 6(a)**), in contrast with the infinite case in **Fig. 1(a)** and ref. [1]. **Fig. 6(b)** shows the calculated pressure as a function of the number of periods using the MST method and the volumetric Lorentz method. For either method, the finite-width results converge to the infinite case as the width increases, as expected.

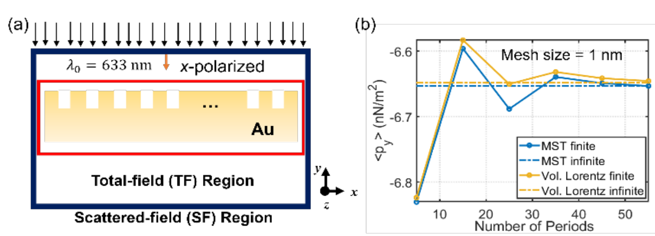

Fig. 6. (a) The finite-width Au structure in free space, illuminated by a plane wave injected at the top boundary of the total-field scattered-field area. The incident field amplitude is the same as that for the infinite-width case. The red box, with all boundaries in free space, is the force-calculation region. (b) The time-averaged optical pressure as

a function of the number of periods, using the MST and volumetric Lorentz methods, compared to the infinite-width case.

Conclusion

We reexamined the time-averaged optical pressure on a corrugated Au film, explored in ref. [1]. We reproduced the calculations and found that, although our calculated optical fields and force densities agree with the published results [1], the resulting steady-state total optical forces are quite different and match the standard radiation-pressure limit, which is the result of momentum conservation of the whole system: the corrugated Au film in free space and the incident and reflected/scattered/transmitted light. The force-enhancement finding in ref. [1] serves as a basis for a later experimental demonstration [5], is related to other published numerical works [2] [3] [4], and has substantial implications for laser sails [28] [29] [30]. Although in this comment we only focus on simulation results in ref. [1], we encourage a reexamination of the results in refs. [2] [3] [4] [5] given the close connection between these works.

Acknowledgements

M. A. K. acknowledges support from the Air Force Office of Scientific Research (FA9550-18-1-0146). Both M. A. K. and V. W. Brar acknowledge additional support from the Breakthrough Initiative, a division of the Breakthrough Prize Foundation.

References

[1] A. H. Velzen and K. J. Webb, Phys. Rev. B **92**, 115416 (2015).
[2] Y.-C. Hsueh, L.-F. Yang, and K. J. Webb, J. Opt. Soc. Am. B, JOSAB **36**, 1408 (2019).
[3] Y.-C. Hsueh, L.-F. Yang, and K. J. Webb, Phys. Rev. B **99**, 045437 (2019).
[4] L.-F. Yang and K. J. Webb, Phys. Rev. B **103**, 245124 (2021).
[5] L.-F. Yang, A. Datta, Y.-C. Hsueh, X. Xu, and K. J. Webb, Phys. Rev. Lett. **122**, 083901 (2019).
[6] M. Mansuripur, Opt. Express, OE **12**, 5375 (2004).
[7] Y. N. Obukhov and F. W. Hehl, Physics Letters A **311**, 277 (2003).
[8] M. Mansuripur, in *Optical Trapping and Optical Micromanipulation X*, Vol. 8810 (International Society for Optics and Photonics, 2013), p. 88100K.
[9] D. B. Phillips, M. J. Padgett, S. Hanna, Y.-L. D. Ho, D. M. Carberry, M. J. Miles, and S. H. Simpson, Nature Photonics **8**, 400 (2014).
[10] K. J. Webb and Shivanand, Phys. Rev. E **84**, 057602 (2011).
[11] K. J. Webb, Phys. Rev. Lett. **111**, 043602 (2013).
[12] D. J. Griffiths, *Introduction to Electrodynamics*, 4th ed (Cambridge: Cambridge University Press, 2017).
[13] J. D. Jackson, *Classical Electrodynamics*, 3rd ed (New York: John Wiley & Sons, 1999).
[14] Q. Ye and H. Lin, Eur. J. Phys. **38**, 045202 (2017).
[15] A. M. Jazayeri and K. Mehrany, Phys. Rev. A **89**, 043845 (2014).
[16] J. Chen, J. Ng, Z. Lin, and C. T. Chan, Nature Photonics **5**, 531 (2011).
[17] P. B. Johnson and R. W. Christy, Phys. Rev. B **6**, 4370 (1972).
[18] B. A. Kemp, Journal of Applied Physics **109**, 111101 (2011).

[19] M. Mansuripur, in *Optical Trapping and Optical Micromanipulation XI*, Vol. 9164 (International Society for Optics and Photonics, 2014), p. 91640B.
[20] S. B. Wang and C. T. Chan, Nature Communications **5**, 3307 (2014).
[21] M. Mansuripur, A. R. Zakharian, and E. M. Wright, Phys. Rev. A **88**, 023826 (2013).
[22] N. Wang, S. Wang, and J. Ng, Phys. Rev. A **97**, 033839 (2018).
[23] S. M. Barnett and R. Loudon, J. Phys. B: At. Mol. Opt. Phys. **39**, S671 (2006).
[24] R. Loudon and S. M. Barnett, Opt. Express, OE **14**, 11855 (2006).
[25] N. A. Mortensen, S. Raza, M. Wubs, T. Søndergaard, and S. I. Bozhevolnyi, Nat Commun **5**, 3809 (2014).
[26] O. Ilic and H. A. Atwater, Nature Photonics **13**, 289 (2019).
[27] D. Van Thourhout and J. Roels, Nature Photonics **4**, 211 (2010).
[28] J. Siegel, A. Y. Wang, S. G. Menabde, M. A. Kats, M. S. Jang, and V. W. Brar, ACS Photonics **6**, 2032 (2019).
[29] H. A. Atwater, A. R. Davoyan, O. Ilic, D. Jariwala, M. C. Sherrott, C. M. Went, W. S. Whitney, and J. Wong, Nature Materials **17**, 861 (2018).
[30] G. A. Swartzlander, J. Opt. Soc. Am. B, JOSAB **34**, C25 (2017).